

Scanning force microscopy investigation of poly(ethylene terephthalate) modified by argon plasma treatment

Ben D. Beake,[†] John S. G. Ling[§] and Graham J. Leggett^{*†‡}

Department of Materials Engineering and Materials Design, The University of Nottingham, University Park, Nottingham, UK NG7 2RD

Contact mode scanning force microscopy of plasma-treated poly(ethylene terephthalate) leads to poor resolution of surface features due to the disruption of delicate structures. However, non-contact mode imaging reveals important new insights into the development of the surface topography with plasma treatment. While the surface wettability reaches a steady state after only a few minutes, SFM reveals subtle topographical developments extending over a period of hours. Using a model polyester containing particulate surface additives, we demonstrate that the rate of erosion of the polymer during plasma treatment may be precisely quantified, and show that at 0.1 mbar Ar pressure, PET is eroded at 4 nm min⁻¹. This high erosion rate persists beyond the point at which the wettability of the polymer has reached a limiting value. Ultimately, the rate of erosion slows. At high treatment times the surface exhibits ridges that align perpendicular to the final draw direction of the film. We speculate that these arise from the preferential erosion of amorphous material.

Introduction

The control of surface chemistry and topography is relevant in numerous applications of polymers in the textiles, adhesives, composites and coatings industries.^{1–6} Many of these applications require good adhesion between the polymer and a surface coating. Typically polymers are hydrophobic and show only limited adhesion to these coatings. There are several methods which can improve the surface hydrophilicity, such as wet chemical processes, and plasma, flame and corona-discharge treatments.⁴ Plasma treatment is an effective method for improving the adhesion and wettability of polymer surfaces whilst leaving bulk properties unaltered. It has the advantage of being non-polluting and ensuring uniform treatment over the sample surface.⁵ In this paper we investigate the relationship between changing surface morphology and wettability under different plasma conditions.

There has been recent interest in the use of scanning force microscopy [SFM] to examine the topographical changes (such as dramatic roughening) which can accompany an improvement in wettability after plasma treatment of polymers such as poly(tetrafluoroethylene),⁷ poly(propylene)^{8,9} and poly(methylmethacrylate).¹⁰ As yet there has been little published work on SFM of plasma treated PET, although Fischer and co-workers have reported scanning electron microscopy [SEM] data showing that whilst oxygen plasma roughens the PET surface, argon plasma does not.¹¹ In the present study we have used SFM to investigate the development of the surface topography of PET films that have been subjected to low power plasma treatments.

In a plasma the surface is exposed to a broad spectrum of ions, electrons, excited neutrals, radicals, UV and VUV radiation.^{2,12} The predominant reactive species in an inductively coupled radio frequency argon plasma are thought to be argon ions and VUV photons which are capable of inducing bond-breaking at the surface forming reactive radicals.^{2,6,12} The relative importance of etching (*via* chain scission), chemical functionalisation (incorporation of polar groups either during

treatment or immediately on exposure to atmosphere) and formation of new surface structures (*via* crosslinking) is not clear.

It was thought that etching might play an important role in the plasma modification of poly(ethylene terephthalate) [PET]. The oxygen functionality on the polymer backbone is a likely weak point,^{13,14} and the role of the ester oxygen in promoting etching has been noted.^{10,13–16} With aromatic groups present the situation may be more complex; the reported stability to degradation of PET over poly(methylmethacrylate) has been rationalised in terms of the ability of the phenyl ring to protect the ester group by various mechanisms.^{14–16} It could be that radicals produced at the ring do not lead to chain scission reactions.¹² The rate of surface etching has been examined using the biaxially oriented PET Mylar D. This material contains silicate additives which are regularly spaced at 0.5–1.0 µm intervals across the film surface. Using SFM we show that the rate of erosion of Mylar D may be quantified accurately and simply. In addition, we wished to determine whether the presence of the additives would affect the surface roughness and orientation in the surrounding polymer matrix after plasma treatment.

On exposure to plasma, a surface may undergo a melting-reorganisation process leading to the formation of large droplet-like features,¹⁷ and the structures observed on plasma-modified samples may not accurately reflect the underlying polymer morphology¹⁸ therefore. However, we provide evidence here, that by using sufficiently mild plasma conditions, such as low power argon plasma, oriented surface features may be produced in PET films that align perpendicular to the final draw direction and which are easily accessible by SFM analysis. This is potentially of considerable use since the properties of PET (*e.g.* toughness, strength) required in several of its industrial applications (*e.g.* fibres, films, laminates) are known to be improved by increasing the molecular orientation.¹⁹ Direct investigation of surface molecular orientation by other methods is confronted by serious experimental problems; however, our data suggest that, with careful control of imaging and surface modification conditions, SFM is able to reveal information about the orientation of material at the film surface.

Experimental

Melinex 'O', a biaxially orientated additive-free PET was obtained from ICI (Wilton, UK) and used as received. SFM

[†]E-mail: Graham.Leggett@umist.ac.uk

[‡]Present address: Department of Chemistry, UMIST, PO Box 88, Manchester, UK M60 1QD.

[§]Present address: British Steel PLC, Welsh Technology Centre, Port Talbot, West Glamorgan, UK SA13 2NG.

and SEM imaging have both shown this additive-free material has a very low surface roughness²⁰ (at μm scale). Mylar D (manufactured by Du Pont, USA), a biaxially orientated PET film treated to incorporate a particulate silicate surface additive, was obtained from Goodfellow Advanced Materials (Cambridge, UK) and used as received. XPS characterisation showed that the films were free of significant levels of contamination.

Plasma treatments were carried out in an inductively coupled radio frequency (13.56 MHz) reactor with a base pressure of 4×10^{-2} mbar. Argon (BOC, special gases, UK) was flowed through the reactor for 15 min before treatment. Plasma treatment was carried out at 0.1 or 1.0 mbar argon pressure and 10 W power. After treatment, the reactor was evacuated down to base pressure before exposing the sample to laboratory atmosphere.

The additive-free Melinex 'O' was used in the wettability study. Static advancing contact angles were measured within 30 min of plasma treatment on a Rame-Hart model 100-00 goniometer using triply distilled water passed through a Millipore 'Milli-Q' purification system. Recorded angles are averages of at least six measurements.

Topographic scanning force microscopy (SFM) images were obtained in ambient conditions with a TopoMetrix Explorer scanning probe microscope (TopoMetrix Corp., Saffron Walden, UK). Contact mode imaging was performed using silicon nitride cantilevers (nominal force constant 0.064 N m^{-1} , nominal tip radius 50 nm) supplied by the microscope manufacturer. The applied force was minimised (typically $< 10 \text{ nN}$) for the contact mode imaging in constant force mode. 'Non-contact' mode imaging was performed using silicon cantilevers. These were obtained from the microscope manufacturer with typical resonant frequencies in the range 130–150 kHz and nominal force constant 50 N m^{-1} (nominal tip radius 20 nm). Imaging was performed in amplitude detection mode with feedback achieved at 50% of the free air resonance amplitude of the cantilevers. 'Non-contact' mode is in fact an intermittent contact mode, in which the tip, oscillated at high frequency and high amplitude, makes frequent contact with the sample surface. However, because these contacts are brief and the tip does not traverse the sample in contact, the frictional interaction between the tip and sample is minimised and hence the imaging process is significantly less disruptive than conventional contact mode imaging. The TopoMetrix Explorer software was used for the surface roughness analysis.

Samples were placed in the plasma reactor with the direction of initial polymer draw relative to the gas flow through the reactor varied between 0 and 90° to investigate whether this had an effect on the nature of the alignment of the surface structures observed at longer treatment times.

Scanning electron microscopy of the plasma-treated films was carried out using a JEOL 6400 scanning electron microscope. Samples were gold-coated (4 nm layer) before use. The accelerating voltage was 15 kV and the working distance 15 mm.

Results

SFM: contact vs. non-contact imaging

Imaging plasma treated surfaces in contact mode with minimal force yielded little topographic information [Fig. 1(a)]. Streaks were observed in the scan direction indicating that the surface is being modified by the action of the tip. In contrast, surface features were imaged clearly using non-contact mode [Fig. 1(b)]. Although tip-sample contacts do occur, the lateral forces that lead to surface wear are minimised. Non-contact mode was therefore used to study the development of topography on plasma treatment.

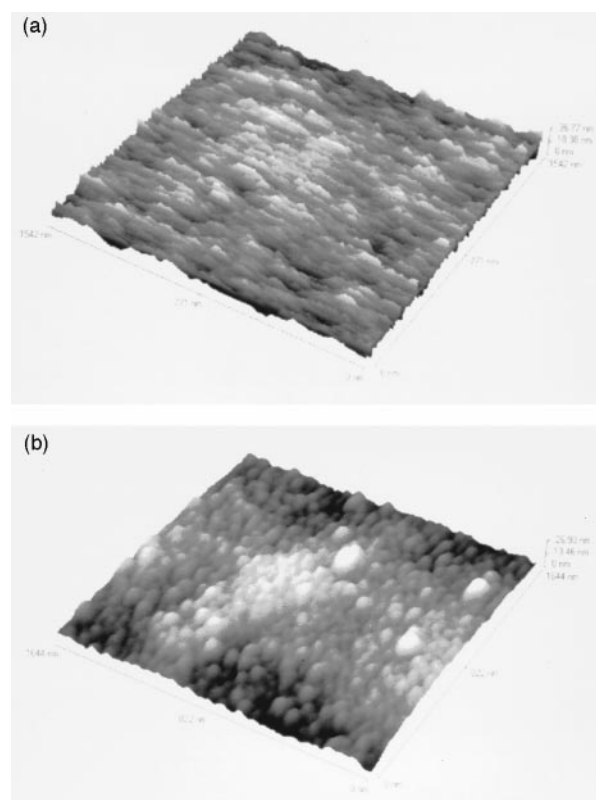


Fig. 1 (a) Contact mode SFM image of plasma treated Melinex 'O'. 1 h 0.1 mbar argon pressure. Scan size: $1.6 \mu\text{m} \times 1.6 \mu\text{m}$. Scan direction is left-to-right across the image. (b) Non-contact mode SFM image of plasma treated Melinex 'O'. 1 h 0.1 mbar argon pressure. Scan size: $1.6 \mu\text{m} \times 1.6 \mu\text{m}$.

Non-contact SFM: development of surface topography on plasma treatment

As-received Melinex 'O' was found to be essentially very flat, having a topography which resembled rolling hills (Fig. 2) with a lateral peak-to-peak distance of around 100 nm. The surface roughness, as measured by the variance of the root-mean-square (RMS) height of the surface features, was quite low, $(4 \pm 1) \text{ nm}$ for a $3 \mu\text{m} \times 3 \mu\text{m}$ area. Some surface scratches (presumably from the manufacturing process) were visible at lower magnification.

After plasma treatment for 1, 10 and 20 min (0.1 mbar Ar; 10 W) a change in the surface topography was observed [Fig. 3(a)]. The sizes of the hills appeared less regular and smaller though the roughness (as defined above) was unchanged and the z (vertical) scales in Fig. 3 (a)–(c) are very similar. The lateral peak-to-peak distance changed from over

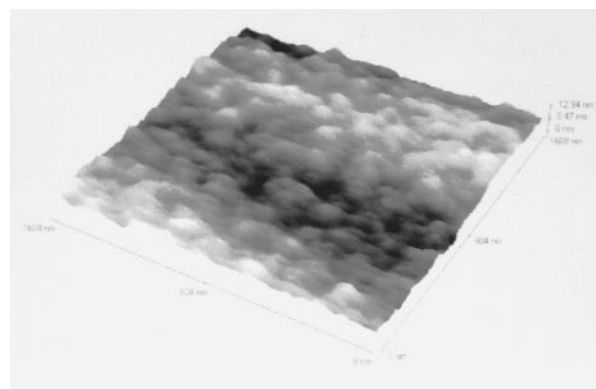


Fig. 2 Non-contact mode SFM image of untreated Melinex 'O'. Scan size: $1.6 \mu\text{m} \times 1.6 \mu\text{m}$.

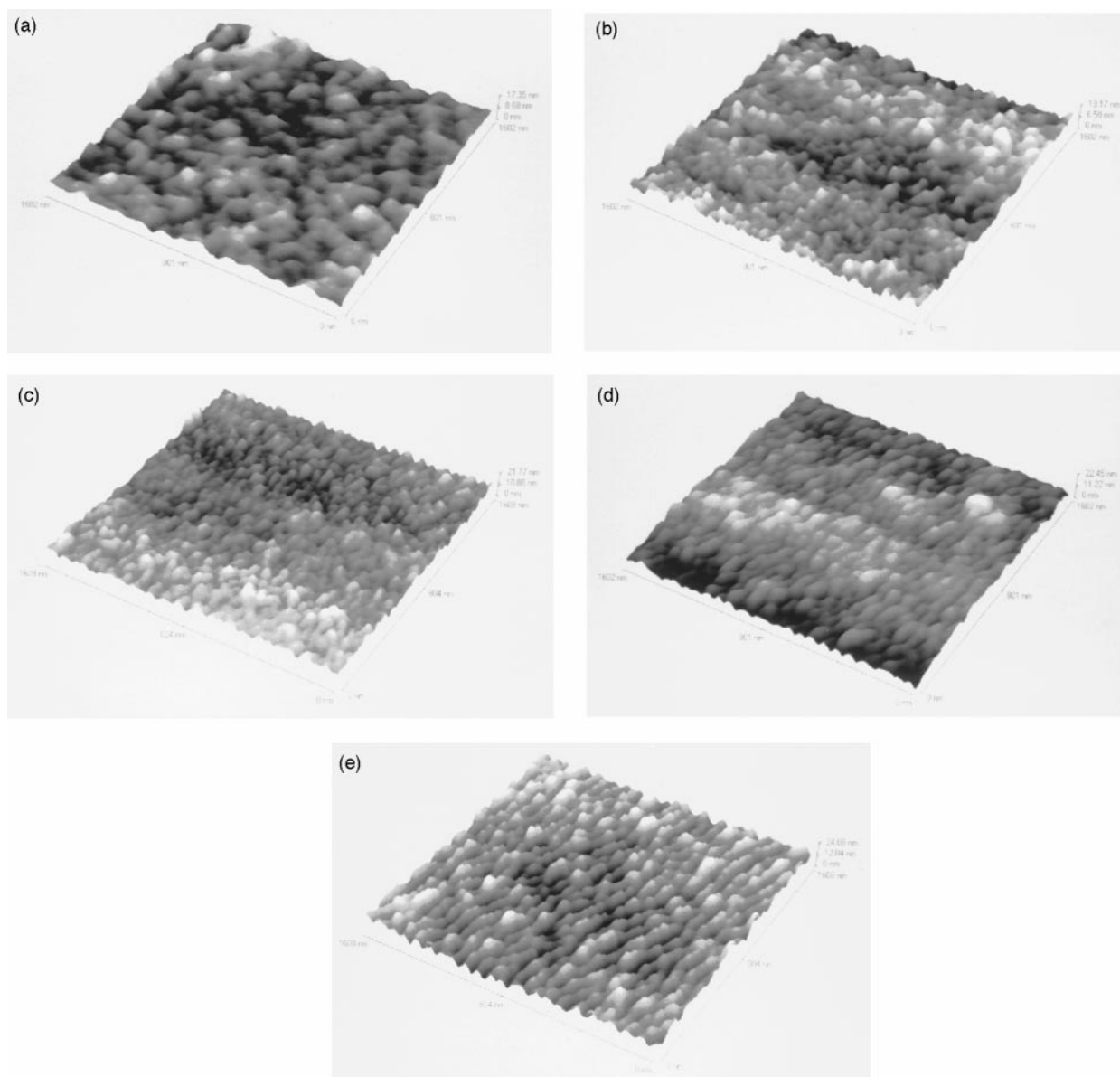


Fig. 3 Non-contact mode SFM image of plasma treated Melinex 'O'. 0.1 mbar argon pressure; (a) 1 min, (b) 10 min, (c) 20 min, (d) 60 min, (e) 90 min treatment. Image size: $1.6 \mu\text{m} \times 1.6 \mu\text{m}$.

100 nm for the gently undulating virgin surfaces to *ca.* 60 nm after 20 min treatment. By 1 h [Fig. 3(d)] the surface features were no longer randomly oriented but exhibited a ridged structure. On treatment for progressively longer times the ridged structure became more pronounced [Fig. 3(e)].

The topographical changes resulting from plasma treatment were not accompanied by a change in surface roughness, as measured by the variance of the RMS height of the surface features, which remained constant at around 4 nm for a $3 \mu\text{m} \times 3 \mu\text{m}$ area, very close to the value determined for untreated Melinex 'O'. Together with the observation that surface scratches, often evident on the untreated material, were absent on plasma treated PET, it may be inferred that the polymer surface is being continually eroded with time. In order to explore this further, the rate of erosion was investigated using Mylar D, a commercial PET with silicate additives embedded into the polymer surface.^{20,21} Fig. 4 compares SFM images of untreated and plasma-treated Mylar D. The z-scale (the vertical scale) is identical in both images to facilitate direct comparison. It can be seen that a significantly greater portion of the additive particles is exposed at the surface following plasma treatment than is exposed in the untreated material. In order to determine the magnitude of the change more

precisely, a quantitative analysis was performed. The top of a given additive particle was selected and its height determined. A nearby point on the polymer surface, equidistant from silicate particles, was then selected and its height determined using the microscope software. The difference was taken to be the height of the additive above the surrounding polymer. The measurement was repeated a large number of times for a number of different samples at each of a number of different treatment times and conditions, and the data plotted in Fig. 5. This quantity was remarkably uniform for the untreated material: an average height of (35 ± 3) nm was determined for the exposed portions of the additive particles. Changes in additive height on plasma treatment were subsequently calculated relative to this. On plasma treatment the heights of the silicate additives above the surface increase greatly as may be seen from Fig. 6, which shows the height of the additive particles as a function of treatment time. This increase is about four times as great at the lower argon pressure used.

Surface orientation on biaxial and uniaxial PET films after plasma treatment

After extended plasma treatment the long-range orientation of the ridged structure could be clearly seen, and within some of

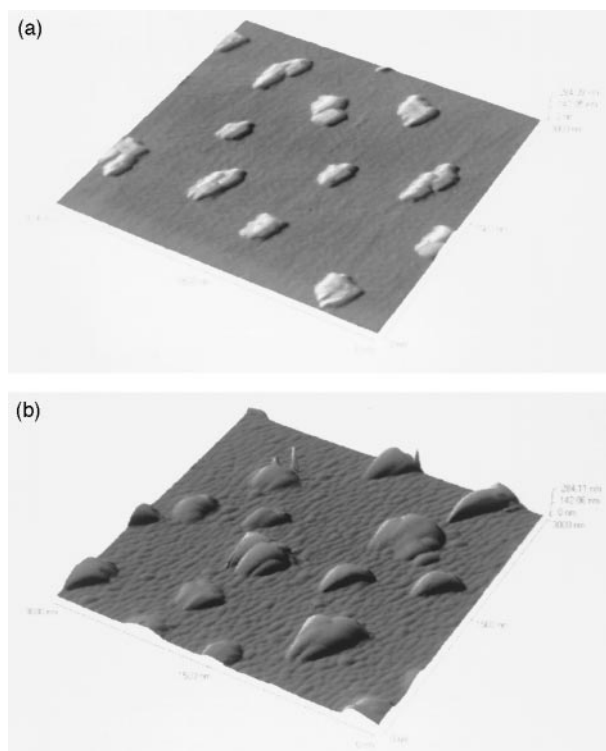


Fig. 4 Non-contact mode SFM images of Mylar D (a) untreated and (b) plasma treated for 2 h at 1 mbar argon pressure. Image size: $3\ \mu\text{m} \times 3\ \mu\text{m}$. The vertical scale is identical in each case and spans 284 nm.

the ridges globular features could be distinguished [Fig. 7(a) and (b)]. By varying the direction of gas flow relative to the direction of initial draw, it was found that, for the biaxially drawn Melinex 'O', the polymer draw direction, rather than gas-flow direction, was the determining factor in the alignment of the ridges. The ridges were always orientated perpendicular to the final, transverse, draw direction regardless of sample positioning in the reactor. This independence of sample structure from the position within the reactor is expected from literature reports⁵ that even complex three-dimensional structures can be uniformly exposed to inductively coupled plasmas. Small deviations ($\pm 5\text{--}10^\circ$) of the apparent alignment probably result from imprecision in our knowledge of the exact draw direction.

In order to further confirm that the ridged structures were not an artifact induced by the imaging process, SEM images were acquired for gold-coated specimens. A representative image is shown in Fig. 7(c). The ridged features are clearly evident in Fig. 7(c), and the globular features identified in the SFM images are also evident. However, the resolution is inferior to that achieved using SFM.

The topography of the plasma treated Mylar D surface between the additives was found to be similar to that of the additive-free biaxial film Melinex 'O' following plasma treatment. In comparison to the plasma treated Melinex 'O' surface, there appeared to be small differences in roughness in the additive-free regions, with the Melinex 'O' surface having lower RMS values. The presence of the additives reduced the long range alignment of the ridged features. In regions without additives nearby, the alignment also appeared to exhibit a shorter range; however the size of the surface features was found to be very similar to the dimensions of those observed on Melinex 'O' after plasma treatment.

The topography of an experimental uniaxially oriented film was also examined following plasma treatment for 2 h, in an attempt to corroborate the result obtained for the biaxially oriented material. The orientation was less clear than in the

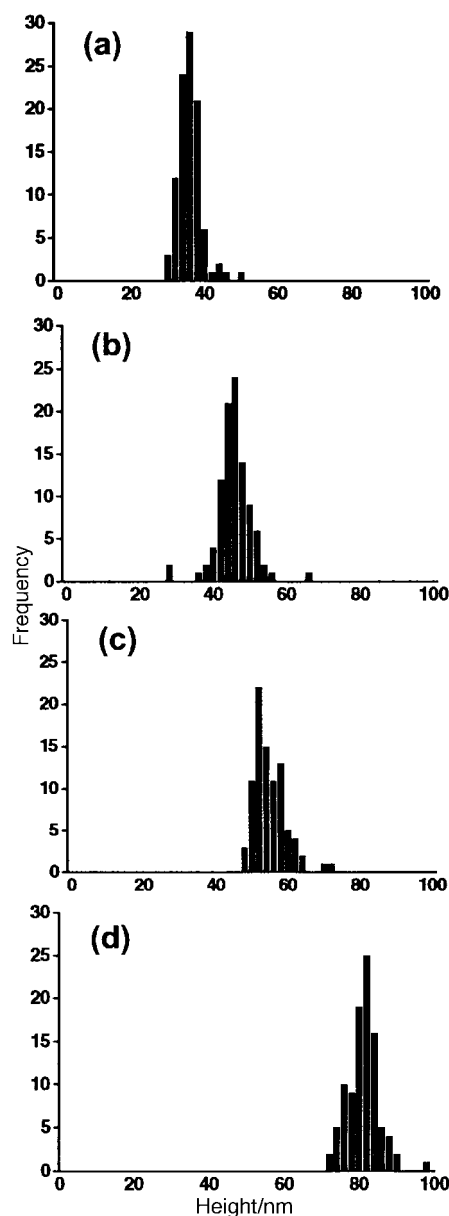


Fig. 5 Histograms showing exposed height of additives above polymer surface for untreated Mylar D (a) and following argon plasma treatment for 10 min (b), 20 min (c) and 60 min (d) at 1.0 mbar

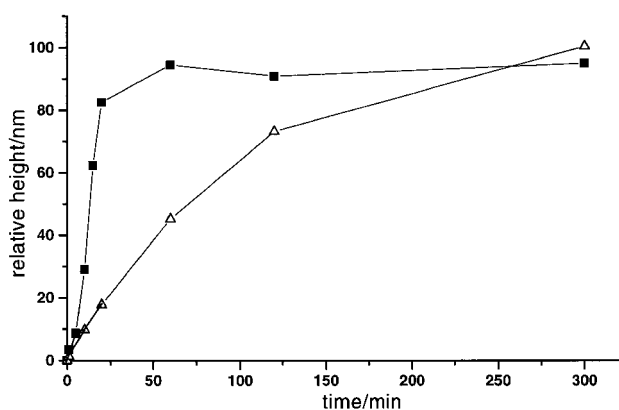


Fig. 6 Increase in additive height above Mylar D surface on argon plasma treatment at 0.1 mbar (filled squares) and 1.0 mbar (open triangles)

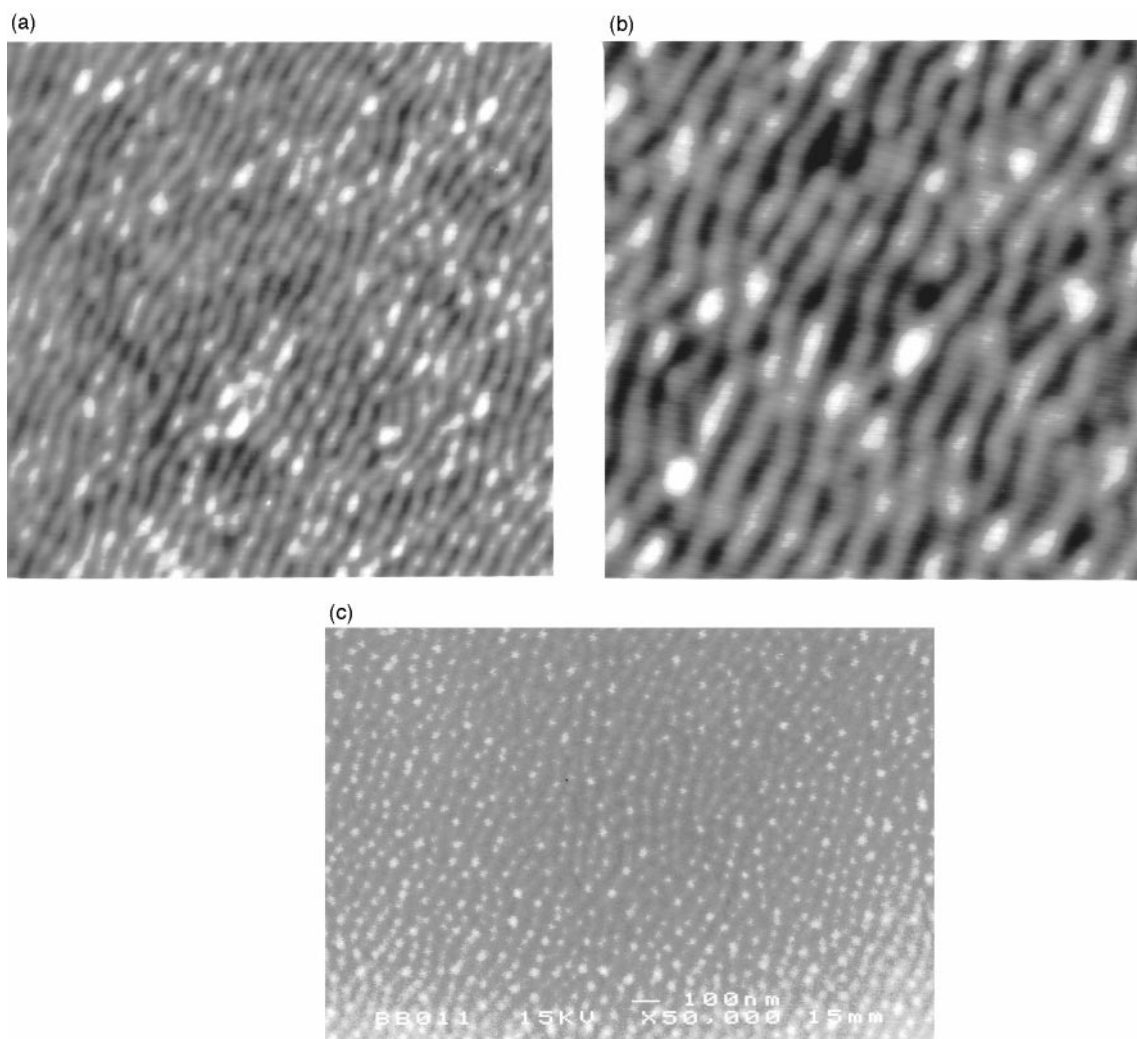


Fig. 7 Non-contact mode SFM and SEM images of the biaxially drawn PET Melinex 'O' after argon plasma treatment at 0.1 mbar pressure for 4 h. (a) SFM, image size $2\ \mu\text{m} \times 2\ \mu\text{m}$ and height scale 14 nm. (b) SFM, image size $1.1\ \mu\text{m} \times 1.1\ \mu\text{m}$ and height scale 13 nm. (c) SEM, 100 nm bar shown. The nominal draw direction is close to the vertical in all three images.

case of the biaxially oriented film, but appeared to be induced perpendicular to the draw direction. However, further work is required to confirm this observation.

Wettability

The advancing contact angle for water on untreated Melinex 'O' was 74° , in acceptable agreement with literature values for PET.^{22–24} The change in wettability by water on plasma treatment can be seen in Fig. 8. The contact angle decreases to a limiting value of $20\text{--}25^\circ$ after about 2 and 5 min

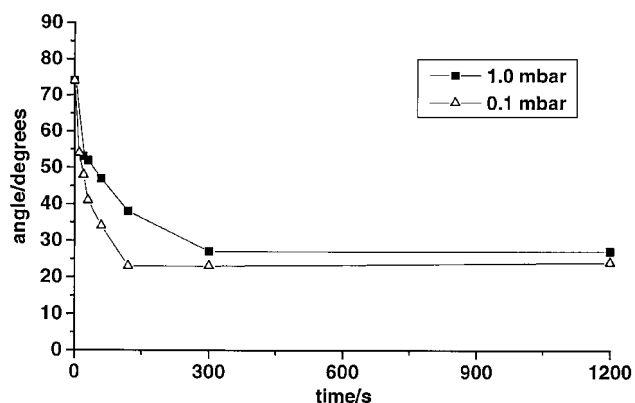


Fig. 8 Variation in water contact angle on argon plasma treatment

plasma treatment at argon pressures of 0.1 and 1.0 mbar respectively. No further decrease is observed at extended treatment times (e.g. for 2 h at 0.1 mbar Ar, $\theta = 21^\circ$). The thermodynamic work of adhesion (W_{sl}) between the polymer and water, calculated from the Young–Dupre equation, [$W_{sl} = \gamma_l(1 + \cos \theta)$], increases from $93\ \text{mN m}^{-1}$ to about $140\ \text{mN m}^{-1}$ on plasma treatment for 5 min or longer. Post-treatment surface ageing occurs and there is some small decrease in wettability with time. Typically the observed water contact angles increased by $10\text{--}20^\circ$ over a five day period after treatment.

Discussion

Comparison of contact and non-contact SFM of plasma-modified PET films

We have previously reported²¹ that low-force contact mode imaging of untreated PET yields essentially the same topographic information as non-contact imaging. It is clear that the untreated polymer surface is not being worn by the action of the tip during imaging at these low loads. Comparison of Fig. 1(a) and 1(b) shows that for plasma-modified PET, in contrast, non-contact imaging provides clearer resolution of topographic data. In contact imaging, the surface was modified in the direction of tip movement during scanning, obscuring the underlying topography. It may be concluded that the plasma-modified material is softer than the untreated polymer,

or that plasma treatment results in the formation of material that is loosely bound to the surface (for example, low molecular weight fragments resulting from partial surface depolymerisation on plasma treatment). This material is more readily disrupted by the tip in contact mode.

A representative SEM image of plasma-treated Melinex 'O' is shown in Fig. 7(c). Although the non-contact SFM images yield clearer resolution of the surface features [Fig. 7(a) and (b)], the similarity of the images obtained by both techniques is clear. The advantages of SFM are in the enhanced resolution and direct access to topographic information, whilst for SEM, the complexity of the image contrast mechanism, and the need for surface pre-treatment mean that the determination of topographical data from the observed contrast is not straightforward.

Rate of surface etching

The results with Mylar D (Fig. 4 and 5) show that etching plays an important part in the plasma modification of PET. The rate of etching is considerably enhanced at the lower argon pressure studied. The mean free path of excited species in the plasma is longer at 0.1 mbar and therefore the probability of species being in an excited state (capable of bond breaking) upon arrival at the surface would be greater.

The initial slope of the plots (Fig. 4) at 0–20 min was used to obtain an etching rate from changes in the exposed heights of the additives. In this region the plots are close to linear and the standard deviation in feature height remains low. The rates of surface etching so obtained were approximately 1 and 4 nm min⁻¹ at 1.0 and 0.1 mbar argon pressure respectively. Although some caution must be exercised in comparing results from different plasma reactors, this nevertheless compares acceptably with literature values for the rates of polymer surface etching by argon plasma. Gerenser²⁵ has determined an erosion rate of *ca.* 6 nm min⁻¹ at 0.07 mbar argon and 10 W primary power by ellipsometric measurements before and after plasma treatment of polystyrene and bisphenol-A-polycarbonate. From the weight loss measurements of Clouet and Shi⁸ on argon plasma treatment of a model organic material, octadecyl octadecanoate, a value of *ca.* 10 nm min⁻¹ at 0.5 mbar argon and 60 W primary power can be determined. This value is in reasonable agreement with our results since the authors report a quite shallow dependence of the rate of surface etching on primary power for argon plasma.⁸

Exposures to argon plasma at 0.1 mbar pressure beyond 20 min resulted in little increase in the mean feature height. The heights of the largest features still increased markedly with time, however, and the variance in observed heights increased dramatically (standard deviations of feature heights typically range from 3–4 nm at short exposure times to 20–40 nm at longer times). Under these more severe conditions the silicate additives may also suffer some damage. The lack of increase in surface roughness on plasma treatment of Melinex 'O' can be explained by surface erosion. The continual etching of the polymer surface may help dissipate some of the temperature increase and avoid the considerable surface roughening often noted on plasma treatment.^{5,11,15}

Surface orientation revealed on biaxially and uniaxially drawn PET films after plasma treatment

A wide range of techniques are currently being employed to determine the effects of the drawing process on the bulk properties of polyester films such as orientation, thermal stability and mechanical strength. Control of these properties is crucial in many of the industrial applications of PET. Data on uniaxially drawn PET film obtained using crystallographic techniques and TEM on ultramicrotomed samples²⁶ have shown that after drawing, the molecular axes of the polymer chains are aligned parallel to the draw, or machine, direction

[MD] and the long faces of the crystallites are perpendicular to it.

Experiments designed to investigate orientation or crystallinity as a function of draw ratio or the speed of the stretching process typically provide data averaged over a wide area, focusing on bulk rather than surface properties. The advantage of SFM imaging is in its surface specificity and access to local variations in topography, orientation and friction.

The data in Fig. 7 clearly show that ridges form perpendicular to the direction of final draw in biaxially drawn PET. The alignment of the ridges, normal to the direction of final draw, is independent of scan direction; the features are not tip-induced. It is clear therefore, that the directionality of the surface features reflects orientation in the film.

Changes in orientation and crystallinity are strongly affected by conditions such as the rate and temperature of draw.²⁷ The thickness of the crystalline core of a lamellar crystallite in uniaxial PET of low volume fraction crystallinity, has been determined as about 5 nm using an electron density correlation function²⁸ to interpret small-angle X-ray scattering (SAXS) results. In comparison, the thickness of the ridges determined in the SFM image in Fig. 7(b) is about 30 nm and the peak-to-peak distance is about 50 nm. Convolution of SFM tip shape with the lateral morphology can occur when the feature widths are of comparable size to the radius of the AFM tip used. Bushell *et al.* have shown that, with a tip radius of 40 nm, features 10 nm wide can appear 80 nm in size.²⁹ It is therefore possible that the globular features we observe in the SFM images are short stacks of a few lamellae; however, it is more likely that the variance reflects differences in sample preparation which alter the crystallite size significantly. A thickening of the crystallites during annealing, and the appreciably larger volume fraction crystallinity in our samples would both be expected to lead to larger crystal sizes.

There is another interesting possibility, that in the SFM and SEM images, we are imaging not only the crystalline core but also a surrounding phase of intermediate order. An investigation into the incorporation of dye into PET fibres by Yasuda and co-workers deduced the presence of a non-dyeable amorphous phase surrounding the crystalline core³⁰ consisting of polymer segments with a relatively high degree of order (though not enough to be detected by X-ray analysis) which is not susceptible to plasma etching.

It is of interest to compare the surface features found in this study with those reported on polymer surfaces modified by more powerful techniques such as reactive gas plasma treatment, high power inert gas plasma treatment and atmosphere silent discharge. Under these conditions, a rise in surface temperature on plasma treatment, combined with chain scission and etching, is thought to lead to a type of melting process at the polymer surface producing low-molecular-weight fragments. The surface becomes highly mobile and the broken polymer chains may recombine to form the observed macroscopic structures. This type of 'overtreatment' producing significant quantities of low molecular weight material at the surface has been reported to have a detrimental effect on the adhesive properties of the plasma treated film.¹⁷ Badyal and co-workers have observed 0.5–1.0 μm globular features on the surface of polypropylene after atmospheric silent discharge treatment.¹⁷ In contrast to low power argon plasma which does not alter the *z*-scale roughness,³⁰ both atmosphere silent discharge and oxygen plasma cause polymer surfaces to roughen considerably.³¹ These authors have also reported that oxygen plasma treatments at higher power produce globular features in the range 40–120 nm on a range of aromatic polymers, such as PET.³² Related work in our laboratory³³ has determined that large globular features (typically with diameters of 200–300 nm) form on more powerful argon plasma treatments, using higher plasma powers (40–100 W). In contrast, our SFM data show that, by using the relatively mild

conditions of low power argon plasma, surface features may be created that reveal the orientation present in the polymer film. Some reorganisation at the surface of a low molecular weight material formed by plasma treatment presumably does occur; however the driving force for macroscopic rearrangements is expected to be considerably lower under the less extreme conditions employed in the present study.

The oriented features we observe by SFM of our plasma-etched PET films are similar to the images (by TEM) of surfaces prepared by a novel angular ultramicrotomy technique reported by Gohil and co-workers.²⁶ These authors have shown that a subsequent, transverse, draw reorients the molecular axes predominantly parallel to the transverse draw direction (TD), with the long faces of the crystallites perpendicular to the TD, although the SFM is capable of revealing greater detail. Similar ridged features, interpreted as stacking lamellar crystallites, have been revealed by Fuchs and co-workers in SFM and TEM images of highly stretched melt-drawn polymer surfaces.^{34–36}

Wettability

The polymer surface becomes considerably more wetted by water after a few minutes plasma treatment, though complete wetting is not observed even after prolonged periods. The decrease in water contact angle reflects the incorporation of polar functionalities either during treatment (trace gases such as air and water vapour in the reactor may play some part in the modification process; the role of residual oxygen has been noted elsewhere^{37–39}) or directly on exposure to atmosphere. The observed finite water contact angle is expected since the continual surface etching limits the build-up of polar functionalities. Prat *et al.*¹⁴ have recently reported that the competition between functionalisation and degradation leads to a limit in the maximum surface energy increase possible on plasma treatment of several polymers and model systems. It should be noted that the improvement in wettability shown by contact angle goniometry in Fig. 8 is observed in minutes whereas the observed morphological changes (Fig. 3) are over a much more extended time scale. Formation of larger structures on a longer time scale than that needed to improve wettability has been observed in oxygen and nitrogen plasma treatment of polypropylene.⁵ In that study a detrimental effect on the wettability with extended exposure to plasma was correlated with a continual roughening of the surface observed by SEM.

The surface structures revealed by plasma treatment of PET in this study appear permanent; SFM images acquired several months after plasma treatment show the rippled morphology remains. However, on a molecular scale some surface reorganisation may occur over a much shorter period. Although slow adsorption of atmospheric contaminants cannot be ruled out, the observed rise in water contact angles over a 5 day period after treatment may suggest that high energy polar groups are being slowly buried below the top 5–10 Å thought⁴⁰ to determine wetting behaviour.

Conclusions

Contact mode SFM of plasma-treated surfaces gave poor resolution of surface topography due to tip-induced movement of low-molecular weight material produced during treatment, whilst non-contact imaging revealed the polymer surface changes from a topography which resembles rolling hills to an orientated, ridged structure. We speculate that these oriented features are composed of crystallites, exposed by preferential etching of amorphous material, and their direction reflects orientation imposed by drawing during film production. This can most clearly be seen in images of the biaxially drawn

Melinex 'O', where the rippled features align normal to the final direction of final draw.

While the surface wettability reaches a steady state after only a few minutes, SFM reveals subtle changes to the surface topography extending over a period of hours. Using a model polyester containing particulate surface additives (Mylar D), we demonstrate that the rate of erosion of the polymer during plasma treatment may be precisely quantified, and show that at 0.1 mbar Ar pressure, PET is eroded at 4 nm min⁻¹. This high erosion rate persists beyond the point at which the wettability of the polymer has reached a limiting value, before it eventually reaches a limiting value.

The authors are grateful to the EPSRC (grant GR/K/88071) and the Royal Society for financial support. J.S.G.L. thanks the EPSRC for a research studentship. G.J.L. thanks the Nuffield foundation for a Science Research Fellowship. The authors are grateful to J. C. Bussey for help in obtaining the SEM image. The authors would also like to thank Professor D. Briggs (ICI, Wilton) for supplying Melinex 'O' with known orientation and for helpful and stimulating discussions.

References

- 1 E. M. Liston, L. Martinu and M. R. Wertheimer, *J. Adhes. Sci. Technol.*, 1993, **7**, 1091.
- 2 E. M. Liston, in *The Interfacial Interactions in Polymer Composites*, ed. G. Akovali, Kluwer Academic, London, 1993, p. 223.
- 3 A. M. Mayes and S. K. Kumar, *MRS Bull.*, 1997, **22**, 43.
- 4 F. D. Egitto and L. J. Matienzo, *IBM J. Res. Develop.*, 1994, **38**, 423.
- 5 K. Harth and H. Hibst, *Surf. Coat. Technol.*, 1993, **59**, 350.
- 6 F. Denes, *Trends Polym. Sci.*, 1997, **5**, 23.
- 7 J. A. McLaughlin, D. Macken, B. J. Meenan, E. T. Mc Adams and P. D. Maguire, *Key Eng. Mater.*, 1995, **99–100**, 331.
- 8 J. F. Friedrich, W. Unger, A. Lippitz, T. Gross, P. Rohrer, W. Saur, J. Erdmann and H-V. Gorsler, *J. Adhes. Sci. Technol.*, 1995, **9**, 575.
- 9 A. Ringenbach, Y. Jugnet and Tran Minh Duc *J. Adhes. Sci. Technol.*, 1995, **9**, 1209.
- 10 P. Gröning, M. Collaud, G. Dietler and L. Schlapbach, *Vide Couches Minces*, 1994, **272**, 140.
- 11 G. Fischer, A. Haemeyer, J. Dembowski and H. Hibst, *J. Adhes. Sci. Technol.*, 1994, **8**, 151.
- 12 R. M. France and R. D. Short, *J. Chem. Soc., Faraday Trans.*, 1997, **93**, 3173.
- 13 F. Clouet and M. K. Shi, *J. Appl. Polym. Sci.*, 1992, **46**, 1955.
- 14 R. Prat, M. K. Shi and F. Clouet, *J. Macromol. Sci. A: Pure Appl. Chem.*, 1997, **34**, 471.
- 15 M. Collaud Coen, G. Dietler, S. Kasas and P. Gröning, *Appl. Surf. Sci.*, 1996, **103**, 27.
- 16 M. Collaud, P. Gröning, S. Nowak and L. Schlapbach, *J. Adhes. Sci. Technol.*, 1994, **8**, 1115.
- 17 D. Boyd, A. M. Kenwright, J. P. S. Badyal and D. Briggs, *Macromolecules*, 1997, **30**, 5429.
- 18 *Polymer Microscopy*, ed. L. Sawyer and D. Grubb, Chapman and Hall, 1987, pp. 111–112.
- 19 A. Aji, J. Guèvremont, K. C. Cole and M. M. Dumoulin, *Polymer*, 1996, **37**, 3707.
- 20 J. S. G. Ling and G. J. Leggett, *Polymer*, 1997, **38**, 2617.
- 21 J. S. G. Ling, G. J. Leggett and A. J. Murray, *Polymer*, in press.
- 22 Y. H. Hsieh and M. P. Wu, *J. Appl. Polym. Sci.*, 1991, **43**, 2067.
- 23 R. A. Hayes and J. Ralston, *Colloids Surf. A, Physicochem. Eng. Asp.*, 1993, **80**, 137.
- 24 C. J. van Oss, R. J. Good and M. K. Chaudhury, *Langmuir*, 1988, **4**, 884.
- 25 L. J. Gerenser, *J. Vac. Sci. Technol. A*, 1990, **8**, 3682.
- 26 H. Chang, J. M. Schultz and R. M. Gohil *J. Macromol. Sci. B: Phys.*, 1993, **32**, 99.
- 27 K. H. Lee and C. S. P. Sung, *Macromolecules*, 1993, **26**, 3289.
- 28 U. Göschel, *Polymer*, 1995, **36**, 1157.
- 29 G. R. Bushell, G. S. Watson, S. A. Holt and S. Myhra, *J. Microsc.*, 1995, **180**, 174.
- 30 T. Okuno, T. Yasuda and H. Yasuda, *Textile Res. J.*, 1992, **62**, 474.
- 31 O. D. Greenwood, R. D. Boyd, J. Hopkins and J. P. S. Badyal *J. Adhes. Sci. Technol.*, 1995, **9**, 311.
- 32 O. D. Greenwood, J. Hopkins and J. P. S. Badyal, *Macromolecules*, 1997, **30**, 1091.

- 33 B. D. Beake, J. S. G. Ling and G. J. Leggett, *unpublished work*.
- 34 L. M. Eng, K. D. Jandt, H. Fuchs and J. Petermann, *Appl. Phys. A*, 1994, **59**, 145.
- 35 H. Fuchs, *J. Mol. Struct.*, 1993, **292**, 29.
- 36 L. M. Eng, H. Fuchs K. D. Jandt and J. Petermann, *Helv. Phys. Acta*, 1992, **65**, 870.
- 37 J. Behnisch, A. Holländer and H. Zimmermann, *Int. J. Polym. Mater.*, 1994, **23**, 215.
- 38 J. Behnisch, A. Holländer and H. Zimmermann, *J. Appl. Polym. Sci.*, 1993, **49**, 117.
- 39 R. Foerch, N. S. McIntyre, R. N. S. Sodhi and D. H. Hunter, *J. Appl. Polym. Sci.*, 1990, **43**, 1903.
- 40 P. E. Laibinis, C. D. Bain, R. G. Nuzzo and G. M. Whitesides, *J. Phys. Chem.*, 1995, **99**, 7663.

Paper 8/01194J; Received 11th February, 1998